

PROJECT APOLLO

VISIBILITY AND OPTICAL TRACKING STUDIES FOR THE
CONCENTRIC FLIGHT PLAN OF LUNAR ORBIT RENDEZVOUS

Prepared by: Charles E. Manry
Charles E. Manry
Guidance Development Branch

George L. Roland
George L. Roland
Guidance Development Branch

Arthur W. Hambleton
Arthur W. Hambleton
Flight Mechanics Applications Branch

Approved by: Paul E. Ebersole
Paul E. Ebersole
Chief, Guidance Development Branch

Approved by: Monte T. Cunningham
Monte T. Cunningham
Chief, Flight Mechanics Applications Branch

Approved by: Robert G. Chilton
Robert G. Chilton
Deputy Chief, Guidance and Control Division

Approved: Eugene H. Brock
Eugene H. Brock
Chief, Computation and Analysis Division

NATIONAL AERONAUTICS AND SPACE ADMINISTRATION

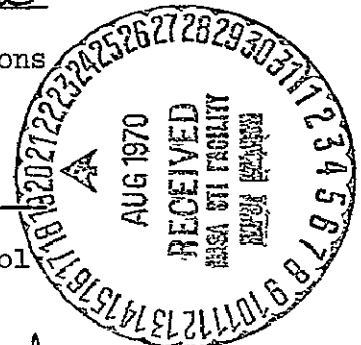
MANNED SPACECRAFT CENTER

HOUSTON, TEXAS

April 20, 1966

N70-35736 (ACCESSION NUMBER)	(THRU)	(CODE)	(CATEGORY)
	5/	21	
7MX-65026 (NASA CR OR TMX OR AD NUMBER)			

FACILITY FORM 602



AUTHOR'S NOTE

The data in this report have been presented in a preliminary form in an earlier paper entitled "Analytical Comparison of Rendezvous Radar and Optical Tracker Systems for Lunar Orbit Rendezvous" prepared by the staff of the Guidance and Control Division. As a result of the numerous reviews, many helpful comments and criticisms were received and are reflected in this report. The mathematical model of the CSM was changed slightly to avoid ambiguity and observations from the GT-8 mission have been incorporated into the analysis of results.

SUMMARY

A digital computer program was developed to evaluate the visibility of the Apollo Command Service Module (CSM) and Lunar Excursion Module (LEM) during lunar orbit rendezvous. Nominal and late launch trajectories of the concentric flight plan type were studied as well as three types of abort trajectories. The results are displayed in the form of time-line bar charts relating the tracking capabilities of the various optical rendezvous guidance sensors.

The sensors considered in this study were:

- a. LEM pilot
- b. LEM optical tracker
- c. CSM scanning telescope
- d. CSM sextant
- e. Manned space flight network

INTRODUCTION

Most of the guidance schemes being considered for use in the lunar orbit rendezvous require some optical or visual tracking of the LEM or CSM by the other vehicle. The proposed optical tracker for the LEM requires a luminous beacon (flashing for purposes of discrimination) on the CSM or passive reflection of sunlight from the CSM surfaces. For manual backup modes of effecting rendezvous, the LEM pilot requires visual tracking to align the LEM window reticle on the CSM. Meanwhile, the astronaut in the CSM will be attempting to track the LEM either by a flashing light or illumination from the sun, being aided in this task by the scanning telescope and sextant.

Because of the number of time-variant factors in the viewing geometry, it was necessary to evaluate the visibility of the vehicles at closely-space intervals during the trajectories. Then by graphically displaying the results in a time-based bar chart format, the regions of reduced tracking coverage can be identified. In addition to providing data on sensor loss-of-track periods for analyses of error propagation, the results of this program may assist in mission planning and crew task-loading studies.

DESCRIPTION OF COMPUTER PROGRAM

Block Diagram

A block diagram of the digital computer program developed for this study is shown in Figure 1. Target and observer vehicle position information as a

function of time is obtained from a separate computer program in the form of time history data cards. A target attitude subroutine is used to orient the vehicles toward each other and to determine the direction of the sun.

The luminous intensity of the target vehicle in the observer's direction is then calculated. Mathematical models of the two vehicles have been developed to simulate the targets. The models include such factors as sun and observer directions, vehicle attitudes, and material reflectances of the vehicles.

For the selected optical aid, the resulting optical gain is used to modify the target intensity to an apparent luminous intensity. In cases where the background behind the target is the sun-lit lunar surface, the lunar surface photometric function (Reference 1) has been used to compute the background brightness.

The apparent luminous intensity of the target is then compared to the tables of contrast thresholds published by Blackwell for the Tiffany Foundation (Reference 2). The result is a visual factor representing the ease of detection.

In the next step, the visual factor is used to find the search time required to locate the target in the field of view of the optical aid. If the search time exceeds some maximum value, the target is considered to be undetected. The computer printout contains information to allow analysis of the reasons for poor tracking coverage.

TARGET DESCRIPTIONS

Sun-Illuminated LEM - An approximation of the luminous intensity of the LEM was obtained by using an equation from Reference 3 for a diffusely reflecting sphere, illuminated by collimated light and viewed from a distance much greater than the radius. Where α is the angle subtended at the sphere between the observer and the light source, the luminous intensity in the observer's direction is:

$$I = \frac{2ER^2}{3\pi} \left[\sin \alpha + (\pi - \alpha) \cos \alpha \right] e$$

I = luminous intensity in candles

E = incident illuminance in lumens/foot²

R = sphere radius in feet

R = sphere radius in feet

α = source-observer angle in radians

e = luminous reflectance of the sphere surface

One of the variables required in the visibility calculations is the projected area of the target which is seen by the observer. In this study, the projected area A for the LEM was found from $A = \pi R^2$. When the range is sufficiently great, the target will subtend less than one minute of arc, which is

the resolution limit of the human eye. Thus, the target will appear as a point source of luminous intensity given by the equation above. At closer ranges where the target can be resolved, the target has been treated as an extended object having a brightness \underline{B} related to the luminous intensity \underline{I} and the area \underline{A} by:

$$B = \frac{\pi I}{A} \text{ (foot-lamberts)}$$

This description of the LEM is not accurate enough to be used in detailed mission planning. It is only used here to demonstrate the effect of the source-observer angle upon the target intensity. Model tests, which have been performed by MIT/IL, show that the luminous intensity exhibits a severe dependence upon LEM attitude relative to the sun direction. A more exact mathematical model of the LEM is presently being developed for use in this program (Reference 4).

Sun-Illuminated CSM - The CSM was assumed to be a cone combined with a cylinder. Reflectance of the cone was assumed to be 0.1 and for the cylinder, a reflectance of 1.0 was used. Both surfaces were assumed to be diffuse reflectors with the luminous intensity of elemental areas dependent only upon the cosines of the angles between the area normal and sun and observer directions.

In order to relate the CSM attitude to the sun and observer directions, the assumption was made that the optics shaft axis line of sight was always directed toward the LEM. To further simplify the analysis, the pitch plane of the CSM was maintained parallel with the plane of the ecliptic. Since the orbital plane was also in the ecliptic plane, the CSM attitude changes required to track the LEM with the optics shaft axis were pure pitch motions. Any other set of assumptions could be used in the program, although more complexity in the vehicle description will result if the pitch plane is not coplanar with the sun and observer.

Appendix I contains the mathematical formulation of the CSM description.

LEM Flashing Light - The flashing light on the LEM is being developed by the Espey Division of Saratoga Industries. The design specification requires that the apparent luminous intensity within the 60° diameter cone be at least 9,000 candles. The lamp consists of a xenon-filled gas discharge tube which is triggered once per second. The pulse duration is about 10 micro-seconds.

Because of radio frequency interference problems, it may become necessary to cover the reflector with a fine-mesh wire screen. This will reduce the luminous intensity of the lamp. For this study, the LEM light intensity was estimated to be 8,000 candles.

CSM Optical Beacon - The CSM optical beacon, being developed by Hughes Aircraft Company for use with the optical tracker, has a visual mode of operation. In this mode, the beacon is switched on for one-half second during each second. Since the pulse repetition rate for the beacon is 32 pulses/second, the beacon will appear as a steady source during the half-second pulse duration.

At the peak of each pulse, the optical beacon is required to produce a radiant intensity of 1.7 watts/steradian. A somewhat higher intensity of 1.94 watts/steradian has been measured on the first engineering model. A value of 2.0 watts/steradian was used in this study.

Assuming that the color temperature of the xenon gas discharge is the same as the 6,000°K color temperature of the sun, the radiant intensity can be converted to the luminous intensity that the average light-adapted human eye would perceive:

$$I_{\text{eye}} = (2.0 \text{ watts/steradian}) \left(680 \frac{\text{lumens}}{\text{watt}} \text{ at } 6,000^{\circ}\text{K} \right) = 1,360 \text{ lumens/steradian}$$

Since the beacon is flashed, its apparent intensity may be increased somewhat over the level which an instrument would measure. The manufacturer claims an advantage from the flashing characteristic of:

$$I_{\text{flash}} = I_{\text{steady}} \left(\frac{t_p + a}{t_p} \right)$$

where t_p = pulse duration in seconds
 $a = 0.2$, Blondel-Rey factor

Thus, the apparent intensity would be 1,904 candles which is the value used in this study.

Optical Aids

LEM Pilot - For the pilot in the LEM, the optical aid is merely the spacecraft window. An estimated window transmittance of 0.9 was used in this study. If the actual transmittance becomes as low as 0.7, the reduction in the detection ranges will be by the factor $\sqrt{0.7/0.9}$, or about 0.9.

At any time when the sun came within 60° of the CSM, no sightings were considered to be valid provided the LEM itself was in sunlight. Experience in Gemini flights has indicated that sun interference does occur; however, the angle limitations for the LEM can only be assumed.

The solid angle in which the LEM pilot was required to search for the CSM was assumed to be a cone with a half-angle diameter of 5° . Rendezvous simulations may be expected to provide the astronauts with the knowledge of where to search at any time during the rendezvous.

CSM Scanning Telescope - The scanning telescope has a 60° field of view and magnifying power of unity. In the rendezvous task, it would be used primarily as an acquisition aid. As an acquisition aid, the scanning telescope offers both advantages and disadvantages compared to an observer looking through a window.

The reticle within the scanning telescope appears to the observer to be located at a great distance away from the spacecraft. It will serve to focus the observer's eye at a distance which will assist the visual search task. Since the optical instruments can be directed by the Apollo Guidance Computer (AGC), the crosshairs of the scanning telescope should be very close to the LEM's position within an estimated 5° at most. If the angular displacement is no more than 0.9° from its predicted position, as guidance error analyses have indicated, the LEM will be within the field of view of the sextant and the scanning telescope will not be needed for acquisition. Because of the numerous optical elements in the scanning telescope, the optical transmission is 0.27 which is roughly one-fourth of the transmission of the LEM window. In addition, the observer using the scanning telescope can only utilize one eye for detection compared to the two eyes of the LEM pilot. The result of this comparison is that the visual detection range of the LEM beacon by the astronaut using the scanning telescope is about the same as that for the CSM optical beacon (one-fourth as powerful) by the LEM pilot.

Sun interference for the scanning telescope was assumed to occur when the sun angle was less than 10° from the edge of the field of view, or 40° from the optical axis.

CSM Sextant - The CSM sextant is a 28 power, 1.8° field of view device. It has an objective aperture of 41 millimeters and an exit pupil diameter of 1.5 millimeters. The optical gain (Reference 5) of such a device can be found from:

$$G = T \frac{D_o^2}{D^2 M^2}$$

provided $D \geq D_o/M$

where T = optical transmission

D_o = objective diameter

D = natural eye pupil diameter when the observer is adapted to the true background brightness without the instrument.

M = linear magnification

If the target is still a point source (less than one minute of arc) after magnification, the optical gain will be:

$$G = T \frac{D_o^2}{D^2}$$

Natural eye pupil diameters at various adaptation brightness levels are shown in Table I (Reference 5). The brightnesses are in millilamberts (1 millilambert = 0.929 foot-lamberts) and the values were used in this study without converting the units. Older observers (above 20 years of eye) experience varying limitations in the maximum and minimum pupil diameters they can achieve (Reference 6).

VISIBILITY CALCULATIONS

Contrast Mode - For cases where the target's subtended angle seen through the optical instrument is greater than one minute of arc and also where the target is viewed against the sun-lit lunar surface, the contrast mode of computing visibility is used. The target luminous intensity I and the visible projected area A are used to find the average target brightness B in foot-lamberts.

$$B = \frac{I}{A}$$

The background brightness B' of the lunar surface was found by:

$$B' = E \Phi$$

where E = mean illuminance of sun at lunar surface, 14,200 lumens/ft²
Φ = lunar photometric function (Reference 1)

Since the lunar photometric function exhibits a strong dependence upon viewing and illuminating angles, the value of B' was computed separately for each time it was required.

The inherent contrast of the target against the sun-lit lunar surface is defined by:

$$C = \frac{B - B'}{B'}$$

When an optical aid is used to view an extended object (greater than one minute of arc subtended angle), the optical gain G must be applied to both

the background and target brightnesses. The result is that the apparent contrast seen through the instrument is the same as the inherent contrast that would be seen without the instrument. The advantage of a magnifying instrument lies in the increased subtended angle of the target. In an actual instrument, some loss of contrast will occur due to scattering of light at the surfaces of the optical elements. This factor may be of importance in the high ambient light levels of outer space but has not been included in this analysis.

Once the apparent contrast has been determined, it is compared to the threshold contrast data obtained by the Tiffany Foundation during World War II. Reference 5 contains a very useful compilation of the data and a description of the experimental methods utilized.

Since the threshold data pertain to a detection probability of 0.5 for a forced-choice temporal experimental method, the threshold contrasts have been multiplied by field factors of 1.2 to convert to "ordinary seeing" and by 1.91 to yield a detection probability of 0.99. When only one eye is used, another factor of 1.414 is used to increase the threshold contrast (see References 5 and 7). The field factors which have been used are lower by a factor of from 5 to 10 than values which are generally used by illumination engineers. The requirement here is to know when sightings might be reliably provided as opposed to knowledge of the one best time to make a sighting, making allowance for all possible degrading factors.

Another consideration, which is a vital part of the rendezvous visibility problem, is the time required to locate the target in the field of view. Both size of the field of view and the ratio of actual contrast to the threshold contrast are involved. The movement of the human eye from one fixation point to the next places a basic time dependence on the search task. Since the sensitivity of the human eye decreases non-linearly with the angle from the foveal axis (fixation center line of sight) and because the dependence varies with the dark adaptation of the eye, the visual search task is nearly impossible to describe quantitatively. In this study, an empirical search equation relating some of these variables has been used. The search times computed from this equation may be in error by a factor of 2 or more in either direction. The search time t in seconds to detect a target with a contrast that is N times threshold in a solid angle Ω steradians is:

$$t = \frac{774 \Omega}{N - 4.12} + 1.0$$

If the solid angle represented by the target exceeded one-fifth of the solid angle of the field of view, the search time was assumed to be 0.5 second.

For all cases where the target was not viewed against the sun-lit lunar surface but was itself sun-illuminated, the point source mode of calculation was used. Also when the target was viewed from a distance sufficient to cause it to subtend less than one minute of arc, the point source mode was used even if the target was viewed against the sun-lit lunar surface.

Whenever a visual target subtends less than one minute of arc to the observer's eye, the target is not resolved by the eye. Visual detection of a point source is dependent upon the total luminous flux entering the eye pupil rather than upon the size and contrast relations which are predominant when the target can be resolved. As a result, the product of target contrast C and the square of the subtended angle θ remains constant. This is known as Ricco's law.

$$C\theta^2 = \text{constant}$$

where $\theta \leq 1$ minute of arc

Making use of this law, the threshold illuminance E_t in lumens/foot² from a point source viewed against a background brightness of B' foot-lamberts, can be found from the contrast threshold data by the relation (Reference 5):

$$E_t = (2.1154 \times 10^{-8}) C B' \theta^2$$

where θ = an arbitrary subtended angle of the target (≤ 1 minute of arc)

C = threshold contrast at background brightness B' of a target subtending the angle θ .

While this technique is considered to be generally applicable at the higher levels of background brightness, the degree of dark adaptation achieved by the astronauts may not be sufficient in real situations to warrant use of a background brightness lower than about 0.01 foot-lamberts. This brightness level is comparable to that of the night sky on earth at full moon. In all cases where the sun-lit moon was not the background, the background brightness was set at 0.01 foot-lamberts.

The search time equation was used in the same way as for the contrast mode. If the search time exceeded 30 seconds for the point source mode and if the background was not the sun-lit lunar surface, the program was arranged to try the flashing light mode.

Flashing Light Mode - The flashing light mode is very similar to the point source mode. The illuminance from the light at the observer's position is computed by the inverse square law. The illuminance threshold is computed in the same way as for the point source mode. However, a different search equation is used for the flashing light. Where N is the ratio of the actual illuminance to the threshold illuminance, Ω is the solid angle in steradians of the field of view, and T is the period of the flash in seconds, the search time t in seconds (Reference 8) is:

$$t = \frac{50 \Omega T}{N - 1} - \frac{T}{2}$$

If N was greater than $(\Omega - .02)/.02$, the search time was set at 0.5 seconds. Both of the lights in this study had periods of one second.

LEM Optical Tracker

Beacon Track Mode - The CSM optical beacon is designed to provide tracking capability for the optical tracker at ranges of at least 400 nautical miles at the minimum intensity points in the beam pattern of the beacon. For this study, the following assumptions have been employed.

Beacon tracking is possible at (see Figure 2):

- a. Ranges up to 400 nautical miles to within 30° of the sun.
- b. Ranges up to 200 nautical miles to within 25° of the sun.
- c. Ranges up to 100 nautical miles to within 5° of the sun.
- d. Intermediate ranges between 100 nautical miles and 400 nautical miles according to a linear relationship between the limits described in a., b., and c.
- e. Ranges up to 40 nautical miles against the sun-lit lunar surface (full moon brightness assumed).

In all cases, the beacon track mode was tried first and only when it failed was the star track mode utilized.

Star Track Mode - The optical tracker is capable of tracking a sun-illuminated CSM (or any other object) provided it is equal in intensity to a third (visual) magnitude star. The point source illuminance from the sun-lit CSM was compared to an illuminance of 1.45×10^{-8} lumens/foot² (Reference 9) to determine if the vehicle could be tracked. Further checks were made to rule out sun interference and sun-lit moon interference by the same criteria as used in the beacon track mode.

RESULTS AND TABULATED DATA

Discussion of Results

General - The results of the study are shown in Figures 3 and 7. Tabulated data, which describe the operating modes of the visibility calculations and the reasons for failure to track, are included in Tables III through VII. In addition to the previously discussed rendezvous sensors, the acquisition and tracking capabilities of the Manned Space Flight Network (MSFN) for the CSM have been included in the figures for each trajectory. Day and night cycles for the LEM have also been shown.

The trajectories, which were selected for study, consisted of three types of aborts prior to landing and two launch cases. The landing and launch trajectories have been summarized below to define the terminology used in the discussion of the results.

After separation from the CSM in an 80 nautical mile altitude circular orbit, the LEM performs a 180° lunar central angle Hohmann descent to an altitude of 50,000'. Then follows a powered descent trajectory ending with the landing of the LEM at the subearth point. The LEM will be launched after a nominal stay time of 36 hours. The powered ascent phase occupies a 10° central angle before injection. The LEM then performs a phasing maneuver at about a 90° central angle from the point of injection. Next, a circularization maneuver places the LEM in a circular orbit close to that of the CSM. Some time later, a transfer phase is initiated in which the LEM changes from its circular orbit to one which intercepts the CSM orbit at the desired rendezvous point.

Table II contains a list of the velocity changes for each of the trajectories which have been analyzed in this study. For the abort cases, the event times begin at separation, while for the launches, the times begin at injection.

The three abort cases are: (1) abort 12 minutes after separation, (2) abort 35 minutes after separation, and (3) abort at the start of powered descent 58 minutes after separation. The nominal launch case includes the 36-hour stay time as does the late launch, which begins at the end of the 200-second launch window.

Since the abort cases occur at approximately the time of landing, the sun angles which have been used for these cases are the extremes of the sun elevation limits proposed for the LEM landing, namely, 15° and 45° above the horizontal at the landing site. The sun azimuth is assumed to be behind the LEM to better illuminate the landing site. As a consequence of the 36-hour stay time, the sun angle will have advanced to 34° and 64° , respectively, from the 15° and 45° elevations at the time of landing. The higher sun angles have been used for the launch cases.

Nominal Launch Trajectory - The data for the nominal launch trajectory is contained in Table III and is presented pictorially in Figure 3. In the 34° sun case, the LEM pilot is unable to detect either the sun-lit CSM or optical beacon for the first 8 minutes after injection. During this period, the range is decreasing from 338 to 291 nautical miles. At 10 minutes after injection, the CSM is no longer sun-lit and the optical beacon again fails to be detectable at a range of 280 nautical miles. Detection does occur at 12 minutes after injection and continues until 54 minutes, using the optical beacon. When the CSM becomes sun-lit again, the sun causes interference to the LEM pilot from 56 to 90 minutes after injection. From 92 to 130 minutes, the sun-lit CSM will be tracked. Beginning at 132 minutes, the optical beacon will be detected as the CSM goes into darkness. Tracking is provided for the next 10 minutes until intercept occurs at 142 minutes after injection.

At the higher sun angle, the LEM pilot will begin to track the CSM using the optical beacon at 12 minutes after injection while the CSM is still sun-lit. CSM darkness occurs at 20 minutes and detection continues through the night phase until 4 minutes after CSM sun rise when sun interference prevents the LEM pilot from detecting the CSM. From 106 minutes until 140 minutes, the sun-lit CSM is detectable. At 142 minutes after injection, the CSM is again in darkness and the optical beacon is used.

The optical tracker maintains continuous track except for the sun interference intervals shown near the circularization maneuver.

At the lower sun angle, the scanning telescope will experience sun interference for the first 8 minutes after injection until the LEM goes into darkness. From then until 14 minutes after injection, the range will be too great for the scanning telescope to provide detection. At a range of about 268 nautical miles, the LEM flashing light will be detected by the astronaut using the scanning telescope. At about 58 minutes, the LEM is viewed against a dark lunar background. Tracking continues until 92 minutes when the LEM will be viewed against the sun-lit moon at a range of 38 nautical miles. Tracking is lost until the range is reduced to 11 nautical miles. The LEM is tracked from then until intercept is accomplished in the darkness of the second orbital night.

At the higher sun angle, range and sun interference prevent tracking until the LEM goes into darkness at about 20 minutes after injection. Tracking is provided for the remainder of the trajectory except while the LEM is viewed against the sun-lit lunar surface.

The sextant provides continuous tracking for both sun angles except for an 8-minute period beginning 10 minutes after injection and a 4-minute period beginning at 136 minutes after injection at the higher sun angle. Sun interference occurs during this interval.

MSFN tracking of the CSM will cover the early portions of the trajectories almost up to the 90° phasing maneuver. The next acquisition will occur just after circularization and good tracking should be available during and after the transfer phase initiation.

Late Launch Trajectory - (See Figure 4 and Table IV) Neither the sun-lit CSM nor the CSM optical beacon are sufficient to provide tracking by the LEM pilot until the range has been reduced from the initial 499 nautical miles to less than 278 nautical miles. This occurs at 46 minutes after injection. The sun interference occurring just after circularization will hinder the LEM pilot in tracking the CSM prior to the transfer phase initiation. However when tracking is regained, the pilot can follow the CSM through the transfer phase to intercept just after the beginning of the second night.

The performance of the optical tracker in this trajectory is particularly interesting. In the beacon track mode, the optical tracker may not track

the CSM beacon beyond 400 nautical miles according to the manufacturer's specification. However if the tracker is shifted to the star track mode prior to the time of LEM injection, the tracker will track the sun-lit CSM as far as 499 nautical miles under the conditions of sun angle and vehicle attitude used in this study. Once beacon mode tracking is possible, however, the tracker should be kept in this mode to reduce the chance of loss of track during the remainder of the trajectory. The range has been reduced to 400 nautical miles at about 18 minutes after injection on this trajectory.

The scanning telescope suffers from sun interference and excessive range problems until the LEM flashing light provides detection at a range of 263 nautical miles. This will occur at 50 minutes after LEM injection. During the interval from 82 minutes until 120 minutes for the lower sun angle, the LEM will appear against the sun-lit moon at ranges from 144 to 23 nautical miles, respectively. Tracking is regained when the LEM is viewed against the dark lunar surface beyond the terminator just before darkness occurs. At the higher sun angle, the same effects occur except that the LEM is detected against the sun-lit lunar surface at a range of 14 nautical miles about 2 minutes before the LEM crosses the terminator into darkness. A brief sun interference occurs at intercept in the higher sun angle case. Since this occurs at just about the time of going into darkness, it is probably not significant.

Sun interference will affect the sextant briefly during the period prior to the 90° phasing maneuver for both sun angles. Otherwise, tracking will be continuous except for the sun interference problem at the higher sun angle near the intercept point.

MSFN tracking is nearly identical to that of the nominal launch.

12 Minute Abort - (See Figure 5 and Table V) For both sun angles considered, the LEM pilot would have sun interference which would prevent tracking of the CSM from about the time of the abort until about the time of intercept. In the lower sun angle case, the LEM pilot would encounter sun interference at 2 minutes after separation.

The optical tracker would be unaffected by sun interference and will provide continuous tracking. Tracking by both the sextant and scanning telescope will be nearly continuous, limited by some sun interference at the time of intercept. On the other hand, MSFN tracking is only available at about 4 minutes prior to intercept.

35 Minute Abort - (See Figure 6 and Table VI) For the lower sun angle, the LEM pilot will not be able to track the CSM because of sun interference except for a 2-minute interval just after separation and a 4-minute interval at intercept. During the 4-minute period beginning 68 minutes after separation, the CSM will not be detected since it will appear against the sun-lit lunar surface at ranges from 28 to 20 nautical miles. A similar effect occurs at the higher sun angle except that the sun's position does not interfere until about 72 minutes after separation. Tracking is allowed from separation until 66 minutes later when the CSM drops below the horizon and is viewed against the sun-lit lunar surface.

The optical tracker and sextant both provide full coverage during this trajectory.

The scanning telescope will not provide acquisition during the period from 16 to 44 minutes at the lower sun angle and from 22 to 44 minutes for the higher sun angle. The LEM appears against the sun-lit lunar surface during this interval at ranges greater than 15 and 25 nautical miles for the lower and higher sun angles, respectively.

MSFN acquisition is completed at the time of the abort and continuous tracking coverage is provided for the remainder of the trajectory.

Abort From the Start of Powered Descent - (See Figure 7 and Table VII) Sun interference at the lower sun angle prevents tracking of the CSM by the LEM pilot from the time of separation until about 10 minutes after the abort. At this time, the CSM beacon will provide tracking for about 4 minutes until the range approaches 282 nautical miles. Tracking is regained using the beacon at 112 minutes after the range has opened to 319 nautical miles and then been reduced to 283 nautical miles. Further loss of track occurs between 160 and 178 minutes while the CSM is viewed against the sun-lit moon at ranges of from 98 to 41 nautical miles. When the range is reduced further, the CSM can be detected against the sun-lit moon at 180 minutes after separation. The sun interference at the lower sun angle near intercept would severely hamper the final phase of LEM rendezvous.

At the higher sun angle, sun interference is nearly absent during the portion of the trajectory prior to the abort. Except for the negligible sun interference at the intercept point, the visibility conditions are much the same as at the lower sun angle for the remainder of the trajectory.

The optical tracker experiences some sun interference following the abort and prior to the 90° phasing maneuver. Also, the excessive range of the CSM beacon when viewed against the sun-lit lunar surface prevents tracking.

The scanning telescope is of little use in this trajectory until about the time of circularization. The brief period of tracking at about 68 minutes after separation is due to the LEM flashing light. Tracking is continuous using various modes for the portion of the trajectories following circularization except for the sun interferences shown.

Other than the sun interference period between circularization and transfer, the sextant experiences only one instance of loss of tracking early in the trajectory at the higher sun angle. The LEM would be viewed against the sun-lit lunar surface from about 22 minutes until 66 minutes after separation. At 62 minutes, the tracking capability becomes marginal and is lost until the LEM rises above the horizon at about 68 minutes after separation. The ranges at 62 and 66 minutes after separation are 203 and 229 nautical miles, respectively.

MSFN tracking coverage covers the abort and 90° phasing maneuver but does not provide data for the circularization and transfer phase initiation.

EVALUATION OF RESULTS

While the results of this study are the logical product of deductive reasoning, the quantitative nature of the data is only intended to be used on a relative basis. Until an adequate experimental program has been completed, the exactitude of these results cannot be established. However, the trends demonstrated by the results should prove useful in procedures planning and for the optimization of the varied factors involved in mission planning. A summary of the worst of the questionable areas is included below:

LEM and CSM Description Doubts - While the shape of the CSM is fairly well described, both its attitude and surface reflection characteristics have been arbitrarily selected to best suit the analysis. The LEM description is too elementary by any standards and will be improved radically in all further studies.

Sun Angle Limits - The sun angle limitations in all instances have been assumed. In the case of the optical tracker, the limits were conservatively set based on experimental measurements. The LEM pilot's sun limitation was estimated rather optimistically but an exact value may not be established until earth orbit missions have revealed the true nature of the window problems.

Search Time Uncertainty - The form of the search time equation for steady (nonflashing) sources actually increases the field factor by a factor in excess of 4.0. Improvement of the accuracy of this equation is a necessity before the borderline between detection and loss of track can be defined.

Stray Lighting - The degrading effects of stray lighting, both inside and outside the spacecraft, have not been considered. Among the anticipated problems are reflected light from the moon (or earth, in earth orbital mission), and possible window or optics coatings from the launch vehicle. Among the physiological problems of vision which may be important are the time delays associated with light or dark adaptation and a phenomenon known as "empty field" myopia. The latter term refers to the possibility of having an observer's eyes focus on the window and fail to see a more distant target.

In spite of the uncertainties noted above, it is possible to apply the techniques described in this report to the relatively few sightings of nearby objects in space. One such sighting during the GT-8 mission involved a detection of the sun-lit Agena vehicle at a range of 76 nautical miles.

Astronaut Scott reportedly made the observation by glancing up from his on-board charts and immediately detecting the Agena vehicle. At that time, the vehicles were about 7 minutes prior to sunset with the sun behind the Gemini spacecraft.

For the assumed conditions of this study, the sun-lit CSM would have been detected at a range of about 130 nautical miles. If we assume that the

broadside view of the Agena produces a luminous signal equal to that from the end-on view of the CSM, it is easy to understand why the Agena was detected immediately after search was begun. This sighting is a qualitative check only for the validation of the techniques used in this study.

Later in the night portion following, Astronaut Scott detected one of the flashing lights of the Agena vehicle at a range of 45.5 nautical miles. The light detected had an apparent intensity of 135 candle-seconds, pulsed once per second. Allowing 5% degradation because of the 15° off-center viewing at the time of detection, the intensity would be 129 candles. The illuminance threshold from the methods of this study would be 3.1×10^{-9} lumens/foot². A field factor of 2.29 has been applied. The predicted detection range would be 33 nautical miles for a maximum search time of 30 seconds. If the detection probability field factor is reduced to the 0.5 probability level, the theoretical detection range becomes 46 nautical miles.

CONCLUSIONS AND RECOMMENDATIONS

On the basis of this study, several conclusions can be drawn.

- a. The CSM sextant provides almost complete tracking coverage for all of the trajectories considered. Since the scanning telescope was not generally usable, acquisition by the sextant would be dependent upon the use of the on-board computer to direct the line of sight at the LEM.
- b. The optical tracker does exhibit some interference from the sun; but in the case of the late launch trajectory, the star track mode will allow tracking during the critical early part of the trajectory even though the range exceeds 400 nautical miles.
- c. Low sun angles are generally prohibitive to piloting tasks of the LEM crew members during the abort trajectories considered. The sun interferences shown in the vicinity of intercept are probably the results of the impulsive velocity change maneuvers used in the trajectory program and may not occur in the actual rendezvous maneuvers.

An increase in the intensity of the CSM optical beacon appears to be indicated in order to allow LEM pilot tracking during the late launch trajectory. To increase the range capability by a factor of 2 will require an increase in intensity of 4. Consideration might be given to the use of the LEM flashing light system on the CSM in place of the CSM optical beacon's visual mode.

REFERENCES

1. Willingham, D. E., "The Lunar Reflectivity Model for Ranger Block III Analysis", TR No. 34-664, Pasadena, California, Jet Propulsion Laboratory, November, 1964.
2. Blackwell, H. R., "Contrast Thresholds of the Human Eye", Journal of the Optical Society of America, Vol. 36, No. 11, November, 1946, pp. 624-643.
3. Tousey, R., "Optical Problems of the Satellite", Journal of the Optical Society of America, Vol. 27, April, 1957, pp. 262-263.
4. Neu, J. T.; Dummer, R. S.; Breckenridge, W. T.; and Geanakou, J., "Visibility in Space, Target Description Subroutine", Report No. GD/C-DBE-66-004, San Diego, California, General Dynamics/Convair, April, 1966.
5. Hardy, Arthur C., "Visibility Data and the Use of Optical Aids", MIT/IL Report No. E-1385, July, 1963.
6. Defense Supply Agency, "Optical Design", MIL-HDBK-141, October, 1962.
7. Duntley, S. Q.; Gordon, J. I.; Taylor, J. H.; White, C. T.; Boileau, A. R.; Tyler, J. E.; Austin, R. W.; and Harris, J. L., "Visibility", Applied Optics, Vol. 3, No. 5, May, 1964, pp. 549-598.
8. Middleton, W. E. K., "Vision Through the Atmosphere", Canada, University of Toronto Press, 1958.
9. Hughes Aircraft Company, "Technical Proposal for Development and Production of Exterior Tracking Light", September, 1965.

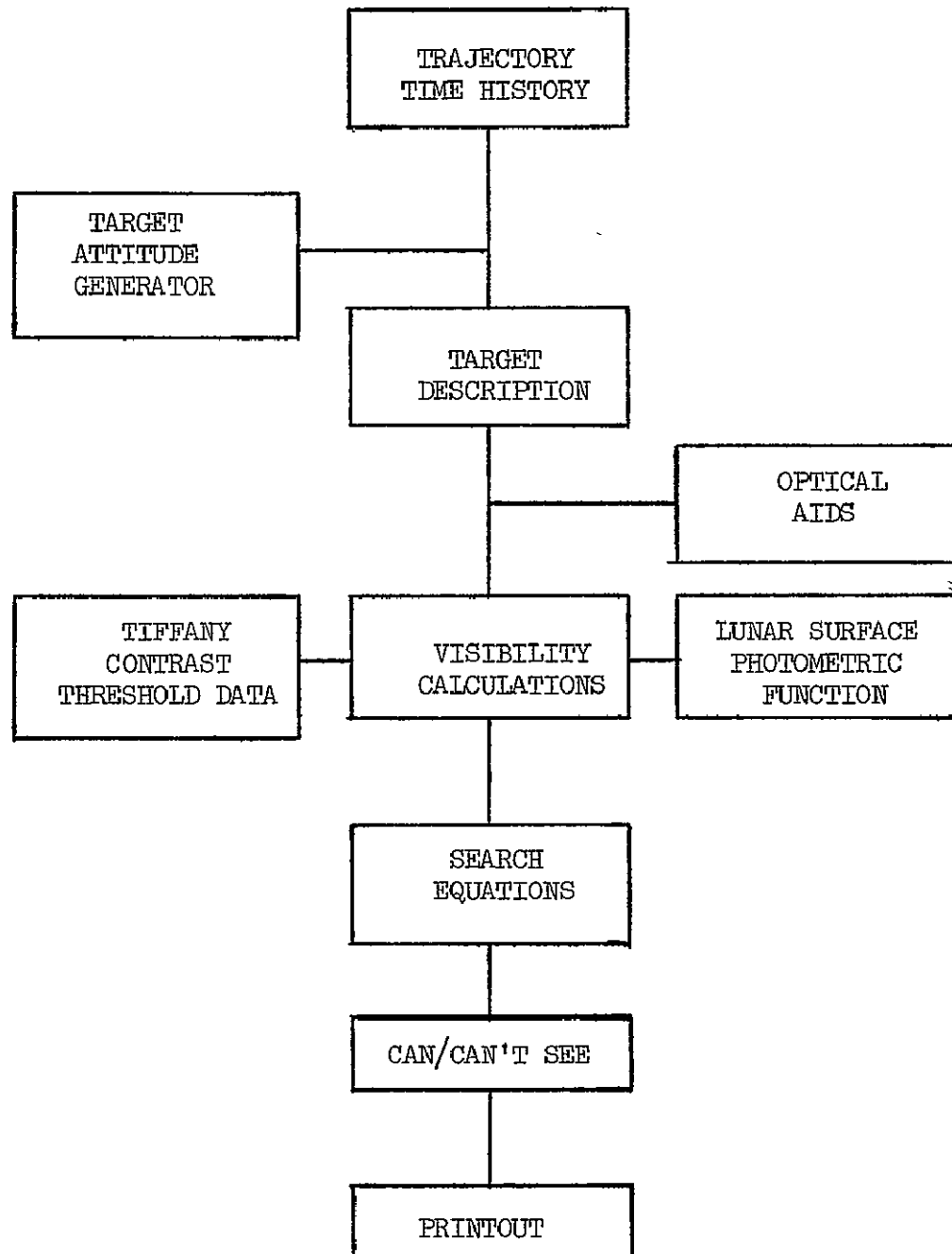


FIGURE 1
BLOCK DIAGRAM OF COMPUTER PROGRAM

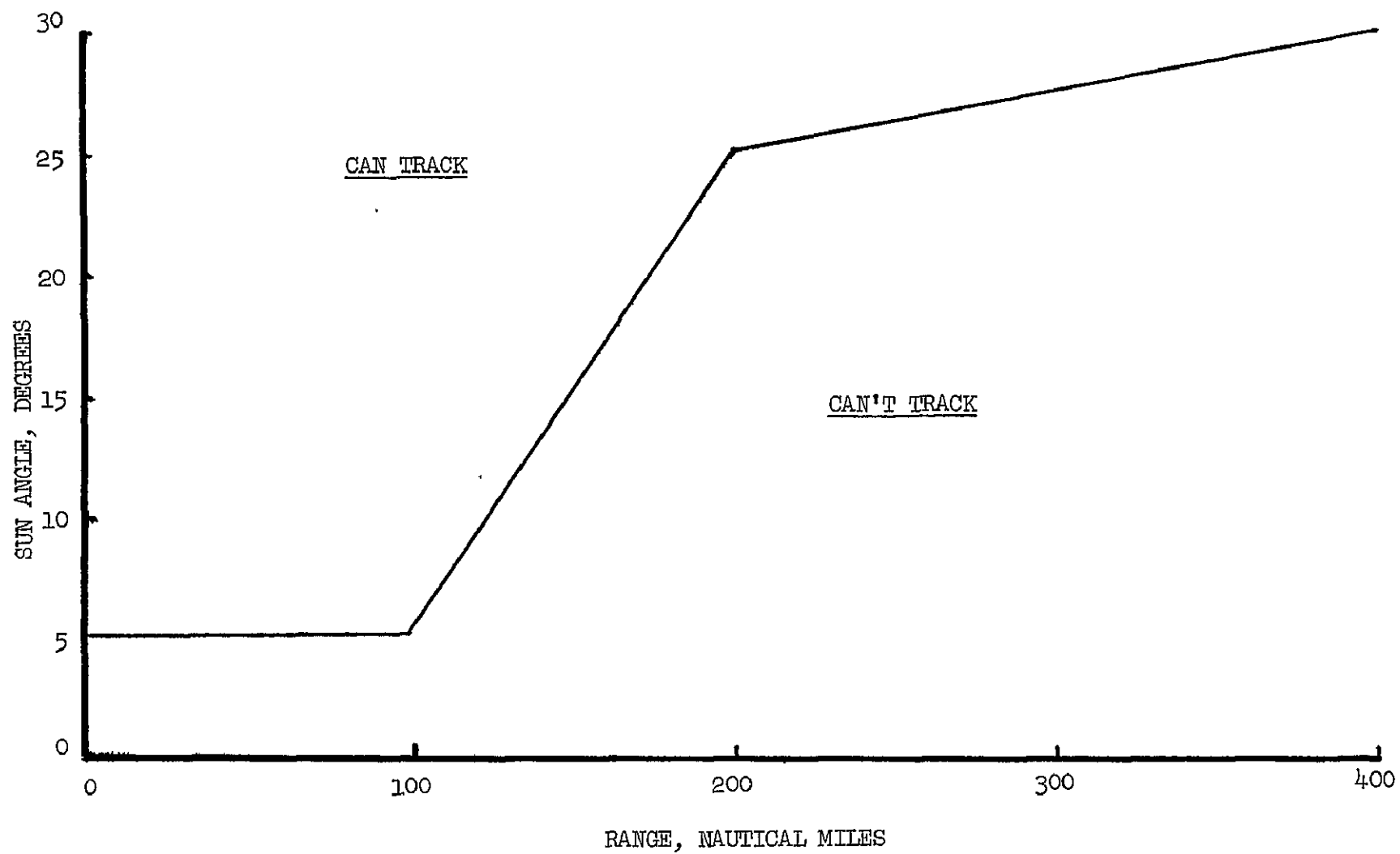


FIGURE 2
LEM OPTICAL TRACKER SUN INTERFERENCE

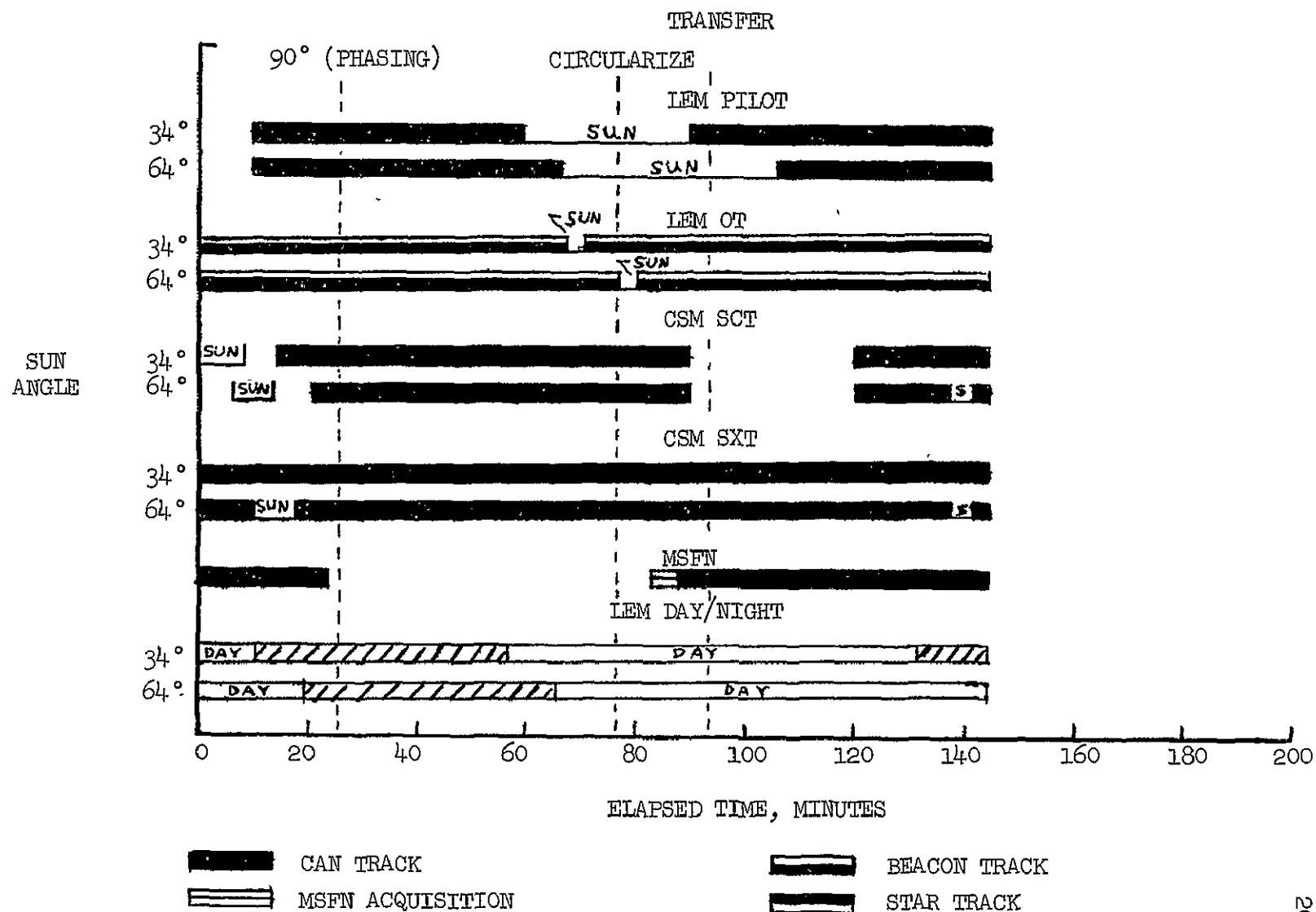


FIGURE 3
VISIBILITY DURING NOMINAL LAUNCH

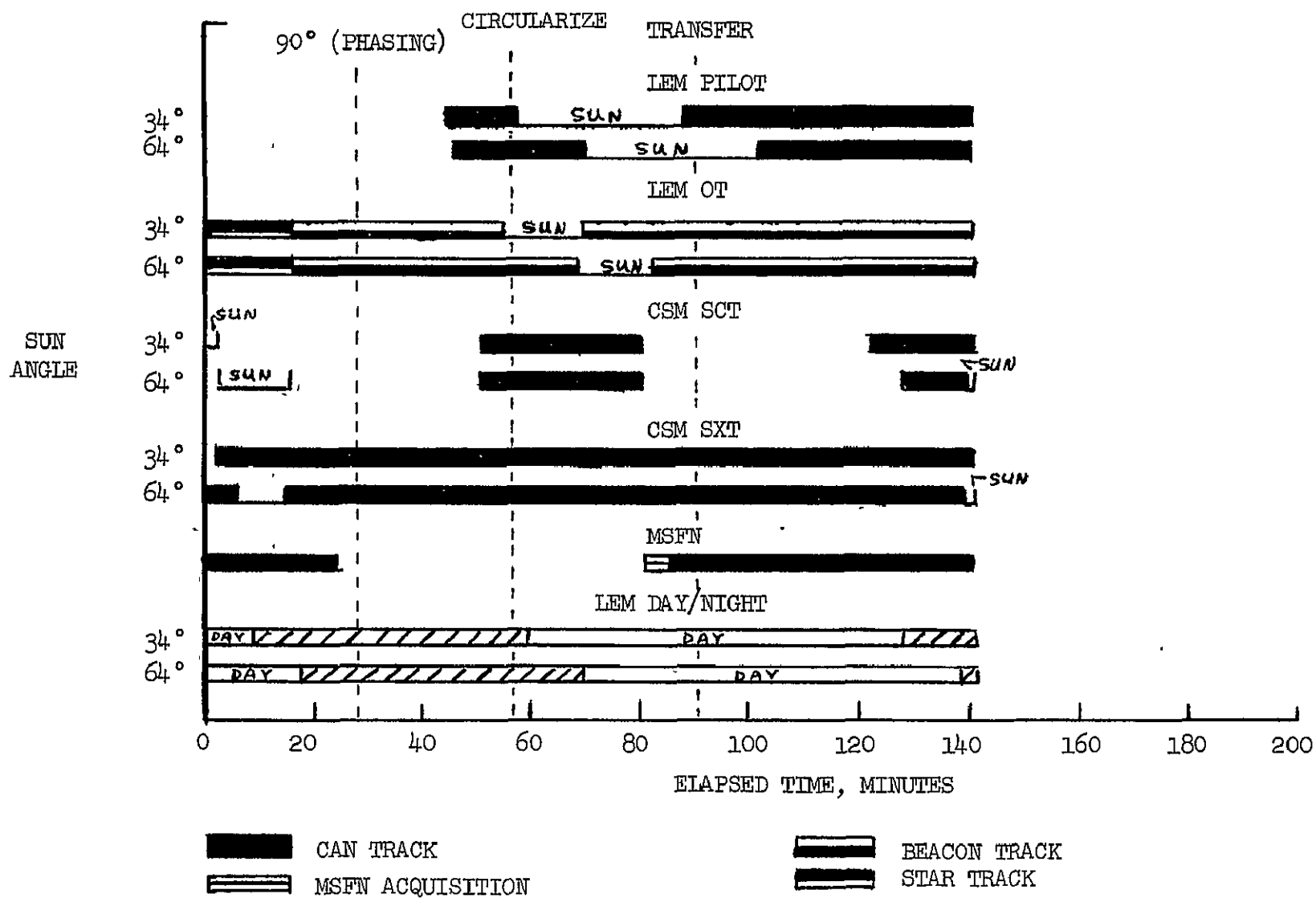


FIGURE 4
VISIBILITY DURING LATE LAUNCH

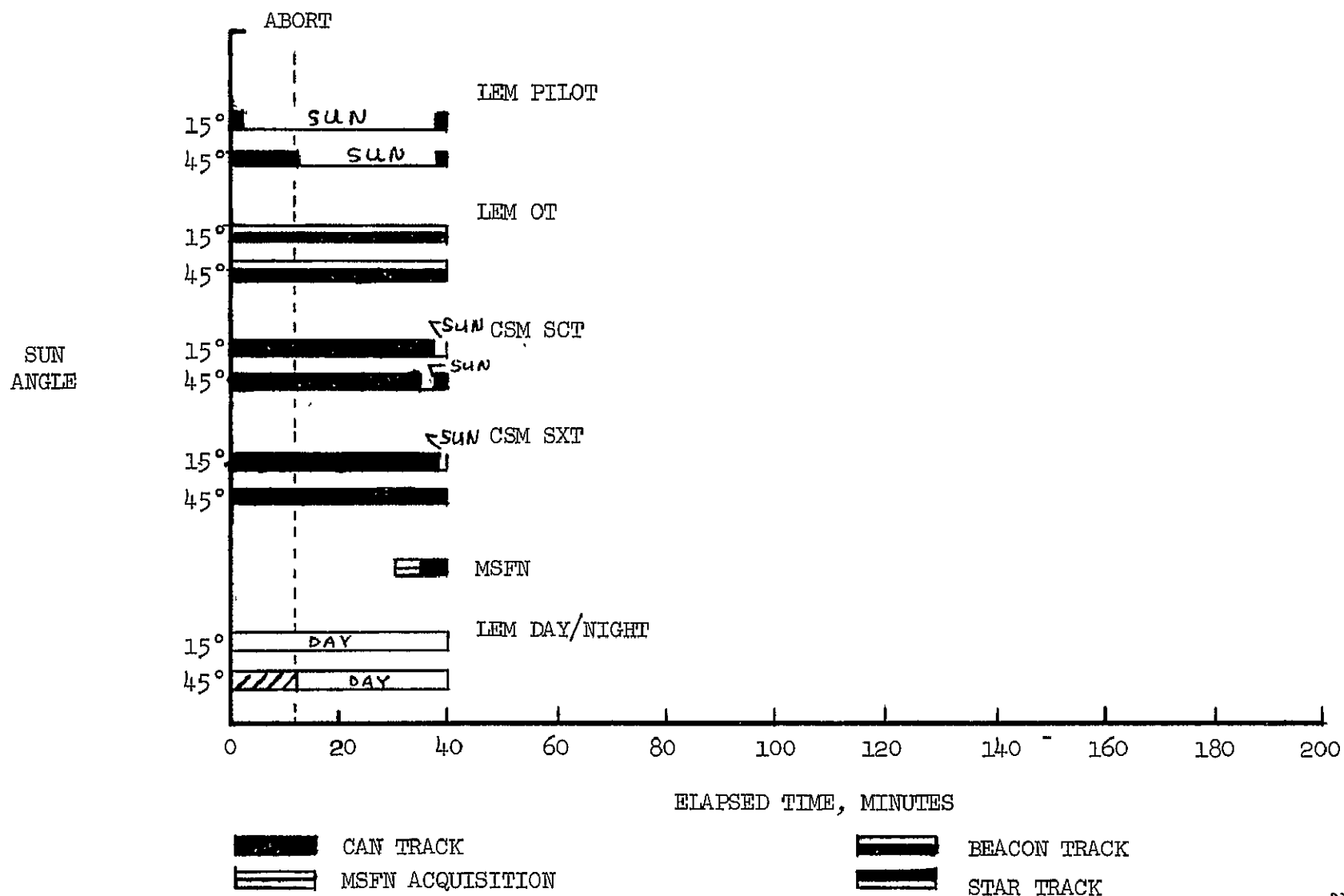


FIGURE 5
VISIBILITY DURING 12 MINUTE ABORT

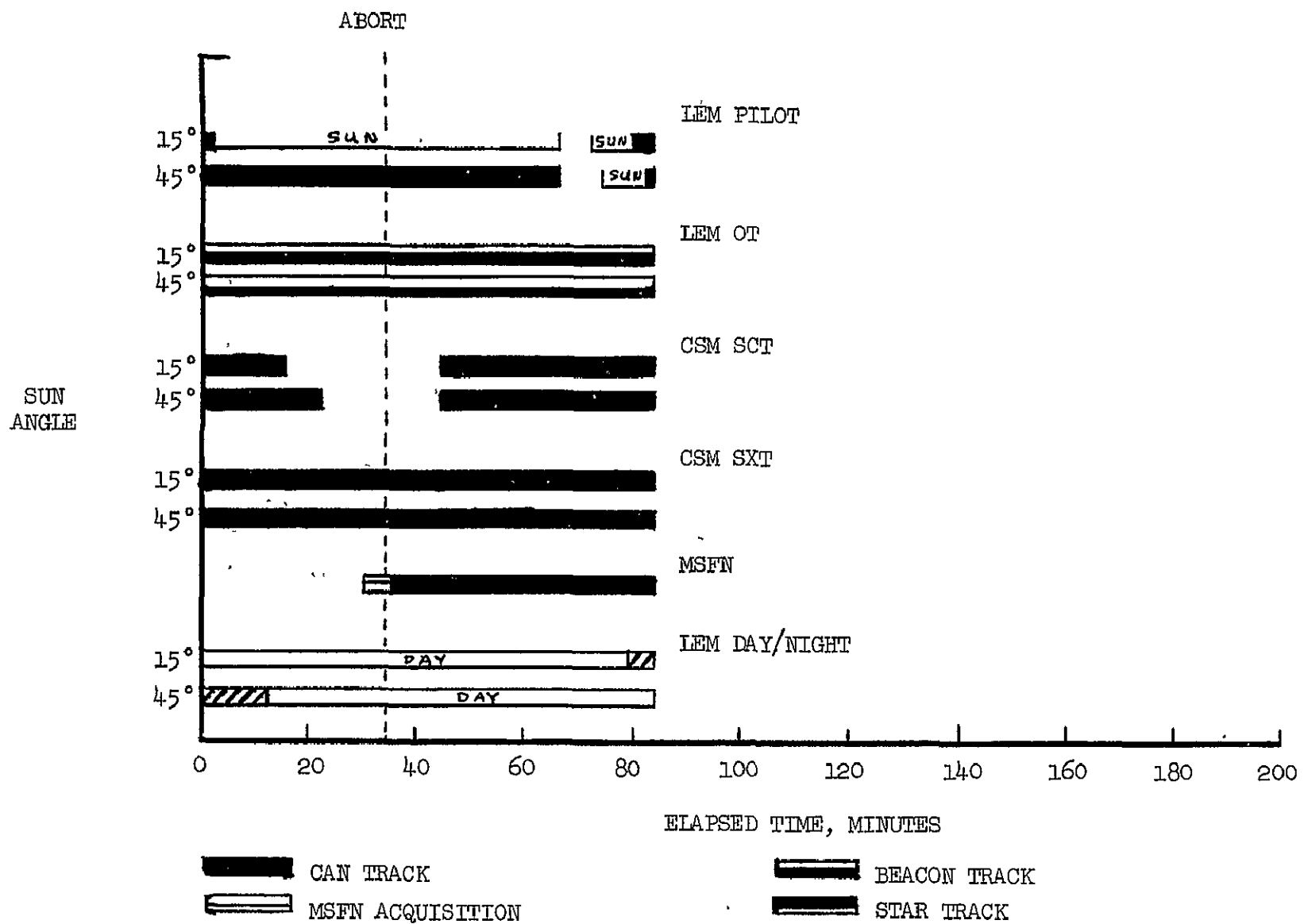


FIGURE 6
VISIBILITY DURING 35 MINUTE ABORT

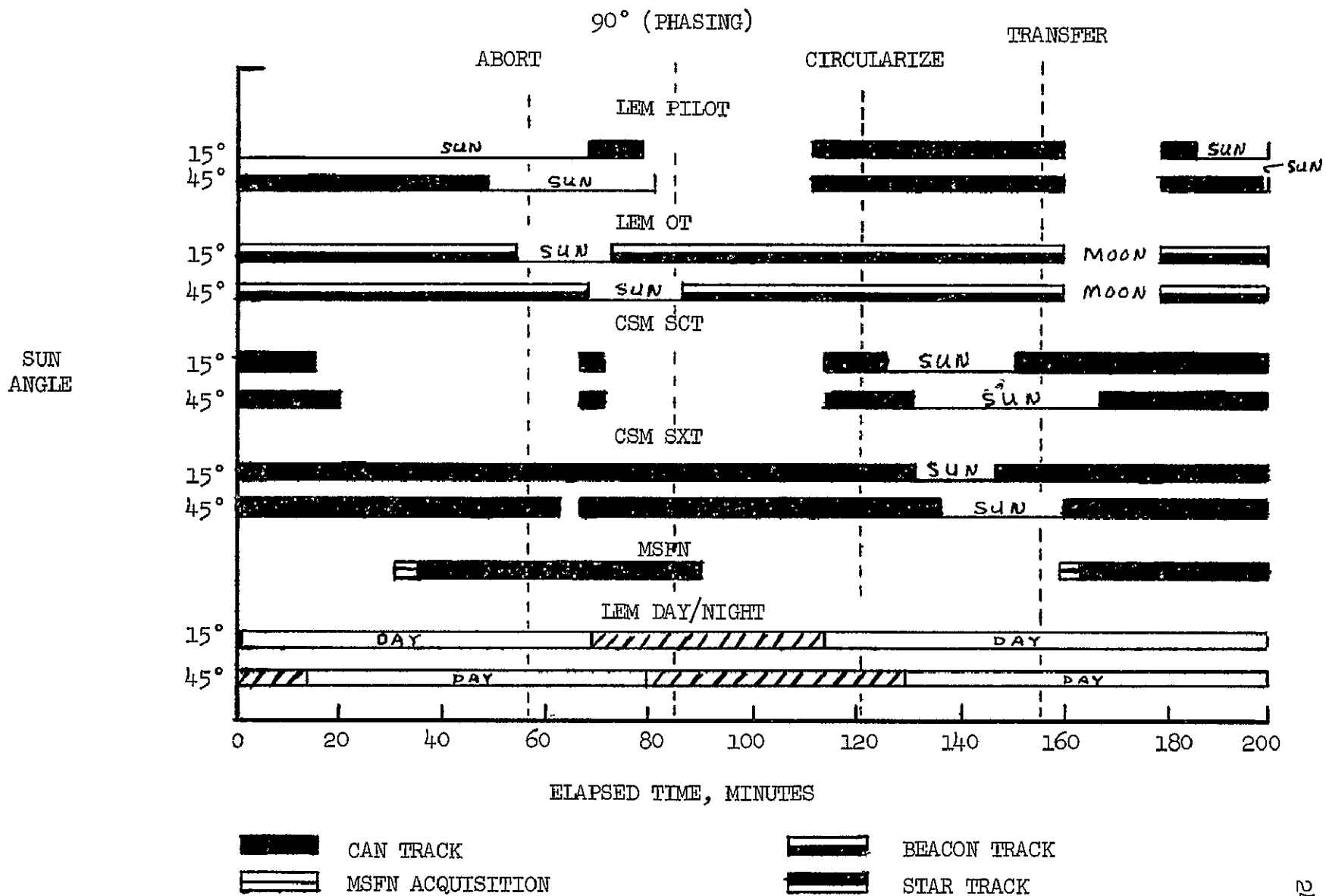


FIGURE 7
VISIBILITY DURING ABORT FROM THE START OF POWERED DESCENT

EXPLANATION OF TERMS

Elapsed time in abort cases is measured from separation and in the launch cases from the end of launch phase.

Tracking (+) indicates the target may be detected within thirty seconds after the beginning of search in the mode of tracking specified. The numbers which follow are the ranges in nautical miles at the beginning and end of the period. If a third number appears in the middle, it is the maximum range during the period.

- + = Target may be detected and tracked.
- R = Range is too great for detection and tracking.
- M = Sun-illuminated lunar surface interferes with optical tracker.
- S = The sun will interfere with tracking if it lies within a minimum angle θ from the target line of sight. The minimum angles assumed for the instruments in this study are:

LEM Pilot $\theta = 60^\circ$

Optical Tracker θ = Range dependent (see Figure 2)

Scanning Telescope $\theta = 40^\circ$

Sextant $\theta = 20^\circ$

Mode of tracking refers to the type of background behind the target in each case as well as the elements involved in visual detection of the target. These have been computer selected for best results.

Star/pt. = The target vehicle is sun-illuminated and appears sufficiently far away to be considered a point source of luminous intensity. Background is the star field.

Moon/pt. = The same as Star/pt. with a sun-lit lunar background.

Dark/pt. = The same as Star/pt. with a dark lunar background.

Moon/ct. = The target vehicle is sun-illuminated and appears sufficiently large that its contrast to the sun-lit lunar background may be used for detection.

Flash = The target vehicle is not sun-illuminated and the background is dark. A flashing light is used.

Star/Flash = Star/pt. mode has been attempted before Flash mode is tried.

Dark/Flash = Dark/pt. mode has been attempted before Flash mode is tried.

Beacon = The optical tracker on the LEM is used in conjunction with the CSM optical beacon.

Star = The LEM optical tracker in the star track mode is used to fix on a steady point source such as the sun-illuminated CSM. This mode was used only if the Beacon mode failed to acquire.

TABLE I

NATURAL EYE PUPIL DIAMETERS AT VARIOUS BACKGROUND (ADAPTATION) BRIGHTNESSES

<u>Adaptation Level</u> (Millilamberts)	<u>Pupil Diameter</u> (mm)
1,000	2.0
100	2.7
10	3.9
1	5.0
0.1	6.0
0.01	6.7

TABLE II

VELOCITY CHANGE SCHEDULES FOR THE ABORT AND LAUNCH TRAJECTORIES OF THIS REPORT

<u>Trajectory</u>	<u>Time</u> (seconds)	<u>Velocity Changes (Feet/Second)</u>		
		<u>\dot{X}</u>	<u>\dot{Y}</u>	<u>\dot{Z}</u>
Nominal launch	1651.9	0	0	-60.3
	4617.8	-30.8	0	59.59
	5805.1	1.52	0	23.6
Late launch	1651.9	0	0	-7.4
	3610.21	-30.902	0	7.373
	5798.99	-3.379	0	82.06
12 minute abort	701.0	149.573	0	48.406
35 minute abort	2101.0	455.542	0	-107.710
Abort from the start of powered descent	3483.0536	-51.5	0	0
	5150.6968	0	0	20.7
	7254.9267	136.6	0	-20.4
	9306.3435	25.0	0	6.0

TABLE III

NOMINAL LAUNCH - Sun Angle 34°

<u>Elapsed Time in Minutes</u>		<u>Mode of</u>	<u>Tracking</u>
<u>From</u>	<u>Through</u>	<u>Tracking</u>	
<u>LEM Pilot</u>			
0	8	Star/Flash	R, 338-291
10		Flash	R, 280
12	54	Flash	+
56	90	Star/Flash	S
92	130	Star/pt.	+
132	142	Flash	+
<u>Optical Tracker</u>			
0	66	Beacon	+
68	70	Beacon	S
72	142	Beacon	+
<u>Scanning Telescope</u>			
0	8	Star/Flash	S
8	12	Flash	R, 291-268
14	56	Flash	+
58		Dark/Flash	+
60	84	Star/Flash	+
86	90	Star/pt.	+
92	118	Moon/pt.	R, 38-11
120	124	Moon/pt.	+
126	130	Dark/pt.	+
132	142	Flash	+
<u>Sextant</u>			
0	8	Star/Flash	S
10	56	Flash	+
58		Dark/pt.	+
60	90	Star/pt.	+
92	124	Moon/pt.	+
126	130	Dark/pt.	+
132	142	Flash	+
<u>LEM Day/Night</u>			
0	8	Day	
10	56	Night	
58	130	Day	
132	142	Night	

TABLE III (continued)
 NOMINAL LAUNCH - Sun Angle 64°

<u>Elapsed Time in Minutes</u>		<u>Mode of</u>	<u>Tracking</u>
<u>From</u>	<u>Through</u>	<u>Tracking</u>	
<u>LEM Pilot</u>			
0	10	Star/Flash	R, 338-280
12	18	Star/Flash	+
20	64	Flash	+
66		Star/Flash	+
68	102	Star/Flash	S
104		Star/pt.	S
106	140	Star/pt.	+
142		Flash	+
<u>Optical Tracker</u>			
0	76	Beacon	+
78	80	Beacon	S
82	142	Beacon	+
<u>Scanning Telescope</u>			
0	4	Star/Flash	R, 338-315
6	14	Star/Flash	S
16	18	Moon/pt.	S
20	66	Flash	+
68	80	Star/Flash	+
82	90	Star/pt.	+
92	118	Moon/pt.	R, 38-11
120	126	Moon/pt.	+
128	134	Moon/ct.	+
136	140	Star/pt.	S
142		Star/pt.	+
<u>Sextant</u>			
0	8	Star/Flash	+
10	14	Star/Flash	S
16	18	Moon/pt.	S
20	66	Flash	+
68	90	Star/pt.	+
92	134	Moon/ct.	+
136		Moon/ct.	S
138	140	Star/pt.	S
142		Star/pt.	+
<u>LEM Day/Night</u>			
0	18	Day	
22	66	Night	
68	142	Day	

TABLE IV

LATE LAUNCH - Sun Angle 34°

<u>Elapsed Time in Minutes</u>		<u>Mode of</u>	<u>Tracking</u>
<u>From</u>	<u>Through</u>	<u>Tracking</u>	
<u>LEM Pilot</u>			
0	4	Star/Flash	R, 499-476
6	44	Flash	R, 464-278
46	50	Flash	+
52	58	Star/Flash	+
60	88	Star/Flash	S
90	128	Star/pt.	+
130	142	Flash	+
<u>Optical Tracker</u>			
0	16	Star	+
18	56	Beacon	+
58	72	Beacon	S
74	142	Beacon	+
<u>Scanning Telescope</u>			
0	2	Star/Flash	S
4	8	Star/Flash	R, 476-453
10	48	Flash	R, 441-263
50	58	Flash	+
60	80	Star/Flash	+
82	120	Moon/pt.	R, 144-23
122	126	Dark/pt.	+
128	142	Flash	+
<u>Sextant</u>			
0	2	Star/Flash	S
4	8	Star/Flash	+
10	58	Flash	+
60	80	Star/pt.	+
82	120	Moon/ct.	+
122	126	Dark/pt.	+
128	142	Flash	+
<u>LEM Day/Night</u>			
0	8	Day	
10	58	Night	
60	126	Day	
128	142	Night	

TABLE IV (continued)

LATE LAUNCH - Sun Angle 64°

<u>Elapsed Time in Minutes</u>		<u>Mode of</u>	<u>Tracking</u>
<u>From</u>	<u>Through</u>	<u>Tracking</u>	
<u>LEM Pilot</u>			
0	16	Star/Flash	R, 499-408
18	44	Flash	R, 397-278
46	60	Flash	+
62	68	Star/Flash	+
70	102	Star/Flash	S
104	138	Star/pt.	+
140	142	Flash	+
<u>Optical Tracker</u>			
0	16	Star	+
18	68	Beacon	+
70	82	Beacon	S
84	142	Beacon	+
<u>Scanning Telescope</u>			
0	2	Star/Flash	R, 499-488
4	16	Star/Flash	S
18	48	Flash	R, 397-263
50	68	Flash	+
70	80	Star/Flash	+
82	126	Moon/pt.	R, 144-14
128	130	Moon/pt.	+
132	138	Dark/pt.	+
140		Flash	+
142		Flash	S
<u>Sextant</u>			
0	4	Star/Flash	+
6	16	Star/Flash	S
18	68	Flash	+
70	80	Star/pt.	+
82	130	Moon/ct.	+
132	138	Dark/pt.	+
140		Flash	+
142		Flash	S
<u>LEM Day/Night</u>			
0	16	Day	
18	68	Night	
70	138	Day	
140	142	Night	

TABLE V
12 MINUTE ABORT - Sun Angle 15°

<u>Elapsed Time in Minutes</u>		<u>Mode of</u>	<u>Tracking</u>
<u>From</u>	<u>Through</u>	<u>Tracking</u>	
<u>LEM Pilot</u>			
0		Flash	+
2	34	Star/Flash	S
36	38	Moon/ct.	+
<u>Optical Tracker</u>			
0	38	Beacon	+
<u>Scanning Telescope</u>			
0		Flash	+
2	6	Star/pt.	+
8	10	Dark/pt.	+
12	20	Moon/pt.	+
22	34	Moon/ct.	+
36	38	Star/pt.	S
<u>Sextant</u>			
0		Flash	+
2	6	Star/pt.	+
8	10	Dark/pt.	+
12	34	Moon/ct.	+
36	38	Star/pt.	S
<u>LEM Day/Night</u>			
0		Night	
2	38	Day	

TABLE V (continued)

12 MINUTE ABORT - Sun Angle 45°

<u>Elapsed Time in Minutes</u>		<u>Mode of</u>	<u>Tracking</u>
<u>From</u>	<u>Through</u>	<u>Tracking</u>	
<u>LEM Pilot</u>			
0	12	Flash	+
14		Star/pt.	S
16	34	Star/Flash	S
36	38	Moon/ct.	+
<u>Optical Tracker</u>			
0	38	Beacon	+
<u>Scanning Telescope</u>			
0	12	Flash	+
14	20	Dark/pt.	+
22	34	Moon/ct.	+
36		Star/pt.	S
38		Star/pt.	+
<u>Sextant</u>			
0	12	Flash	+
14	20	Dark/pt.	+
22	34	Moon/ct.	+
36	38	Star/pt.	+
<u>LEM Day/Night</u>			
0	12	Night	
14	38	Day	

TABLE VI
35 MINUTE ABORT - Sun Angle 15°

<u>Elapsed Time in Minutes</u>		<u>Mode of</u>	<u>Tracking</u>
<u>From</u>	<u>Through</u>	<u>Tracking</u>	
<u>LEM Pilot</u>			
0		Flash	+
2	66	Star/Flash	S
68	72	Moon/pt.	S
74	78	Dark/Flash	S
80	84	Flash	+
<u>Optical Tracker</u>			
0	84	Beacon	+
<u>Scanning Telescope</u>			
0		Flash	+
2	6	Star/pt.	+
8	10	Dark/pt.	+
12	14	Moon/pt.	+
16	44	Moon/pt.	R, 15-56
46	58	Star/Flash	+
60	78	Star/pt.	+
80	84	Flash	+
<u>Sextant</u>			
0		Flash	+
2	6	Star/pt.	+
8	10	Dark/pt.	+
12	44	Moon/ct.	+
46	78	Star/pt.	+
80	84	Flash	+
<u>LEM Day/Night</u>			
0		Night	
2	78	Day	
80	84	Night	

TABLE VI (continued)
 35 MINUTE ABORT - Sun Angle 45°

<u>Elapsed Time in Minutes</u>		<u>Mode of</u>	<u>Tracking</u>
<u>From</u>	<u>Through</u>	<u>Tracking</u>	
<u>LEM Pilot</u>			
0	12	Flash	+
14	66	Star/pt.	+
68	70	Moon/pt.	R, 29-25
72	80	Moon/pt.	S
82	84	Star/pt.	+
<u>Optical Tracker</u>			
0	84	Beacon	+
<u>Scanning Telescope</u>			
0	12	Flash	+
14	20	Dark/pt.	+
22	44	Moon/pt.	R, 22-56
46	60	Star/Flash	+
62	80	Star/pt.	+
82	84	Dark/pt.	+
<u>Sextant</u>			
0	12	Flash	+
14	20	Dark/pt.	+
22	44	Moon/ct.	+
46	80	Star/pt.	+
82	84	Dark/pt.	+
<u>LEM Day/Night</u>			
0	12	Night	
14	84	Day	

TABLE VII
 ABORT FROM THE START OF POWERED DESCENT
 Sun Angle 15°

<u>Elapsed Time in Minutes</u>		<u>Mode of</u>	<u>Tracking</u>
<u>From</u>	<u>Through</u>	<u>Tracking</u>	
<u>LEM Pilot</u>			
0	68	Star/Flash	S
70	74	Star/Flash	+
76	110	Flash	R, 282-319-283
112	124	Flash	+
126	158	Star/pt.	+
160	178	Moon/pt.	R, 98-41
180	192	Moon/pt.	+
194	200	Dark/pt.	S
<u>Optical Tracker</u>			
0	54	Beacon	+
56	72	Beacon	S
74	158	Beacon	+
160	178	Beacon	M
180	200	Beacon	+
<u>Scanning Telescope</u>			
0	2	Flash	+
4	6	Star/pt.	+
8	10	Dark/pt.	+
12	14	Moon/pt.	+
16	64	Moon/pt.	R, 15-216
66		Dark/Flash	+
68		Star/Flash	+
70		Flash	+
72	114	Flash	R, 262-319-266
116		Flash	+
118	124	Star/Flash	+
126	150	Star/Flash	S
152	178	Star/Flash	+
180	200	Star/pt.	+
<u>Sextant</u>			
0	2	Flash	+
4	6	Star/pt.	+
8	10	Dark/pt.	+

TABLE VII (continued)

12	54	Moon/ct.	+
56	64	Moon/pt.	+
66		Dark/pt.	+
68		Star/pt.	+
70	116	Flash	+
118	128	Star/Flash	+
130	146	Star/Flash	S
148	200	Star/pt.	+
<u>LEM Day/Night</u>			
0		Night	
2	68	Day	
70	116	Night	
118	200	Day	

TABLE VII (continued)
 ABORT FROM THE START OF POWERED DESCENT
 Sun Angle 45°

<u>Elapsed Time in Minutes</u>		<u>Mode of</u>	<u>Tracking</u>
<u>From</u>	<u>Through</u>	<u>Tracking</u>	
<u>LEM Pilot</u>			
0	12	Flash	+
14	46	Star/pt.	+
48	78	Star/Flash	S
80	88	Star/Flash	R, 297-316
90	110	Flash	R, 318-283
112	134	Flash	+
136	158	Star/pt.	+
160	178	Moon/pt.	R, 98-42
180	192	Moon/pt.	+
194	198	Moon/ct.	+
200		Moon/ct.	S
<u>Optical Tracker</u>			
0	64	Beacon	+
66	86	Beacon	S
88	158	Beacon	+
160	178	Beacon	M
180	200	Beacon	+
<u>Scanning Telescope</u>			
0	12	Flash	+
14	20	Dark/pt.	+
22	66	Moon/pt.	R, 22-229
68	70	Star/Flash	+
72	80	Star/Flash	R, 262-297
82	114	Flash	R, 303-319-267
116	128	Flash	+
130	164	Star/Flash	S
166	182	Star/Flash	+
184	200	Star/pt.	+
<u>Sextant</u>			
0	12	Flash	+
14	20	Dark/pt.	+
22	60	Moon/pt.	+

TABLE VII (continued)

62	66	Moon/pt.	R, 203-229
68	80	Star/pt.	+
82	128	Flash	+
130	132	Star/pt.	+
134		Star/Flash	+
136	154	Star/Flash	S
156	160	Star/pt.	S
162	200	Star/pt.	+
<u>LEM Day/Night</u>			
0	12	Night	
14	80	Day	
82	128	Night	
130	200	Day	

APPENDIX

CONE-CAPPED CYLINDER ANALYSIS

A very good approximation of the CSM geometry is that of a cone-capped cylinder with the dimensions shown in Figure A-1. In the analysis of this geometry, the cone and cylinder walls will be considered separately. It is assumed that the LEM, CSM centerline, and sun are coplanar. This assumption is not necessary to the analysis but is made here to correspond with the trajectory program. Generalization to the three dimensional case would be straightforward.

The CSM attitude has been assumed to be arranged so that the shaft axis of the optics system was directed toward the LEM. Thus, the LEM is always viewing the CSM from 57° below the +Z axis of the CSM. The CSM communications antenna, optical beacon, and rendezvous radar transponder all have beam patterns which include the shaft axis direction so that this is a fairly reasonable assumption.

The directional reflectance characteristics of the CSM surface materials have not been measured. Diffuse reflection characteristics were assumed for simplicity. Reflectance factors of 1.0 for the cylindrical portion and 0.1 for the conical portion were estimated.

Diffuse Reflection

When a small flat piece of diffuse material is illuminated by a distant source at an angle θ from the surface normal and then viewed from a direction ϕ with the normal, the luminous flux received at a distant location is (see Figure A-2):

$$dF_o = \frac{F_N \cos \theta \cos \phi \, dA}{R^2}$$

where F_N = Incoming luminous flux intensity as measured normal to the flux lines.

θ = Angle of incidence.

ϕ = Angle between the normal to the surface and a line to the observer.

R = Distance from the sample to the observer.

dA = Area of the sample.

Analysis of the Cone

Collimated light is incident from the direction defined by the unit vector (\hat{I}_i) which is given by (Figure A-3):

$$\hat{l}_i = \hat{j} \cos \beta - \hat{k} \sin \beta \quad (1)$$

where β is the angle between the sun and the -Y axis. The observer is in the direction defined by the unit vector (\hat{u}) given by:

$$\hat{u} = \hat{j} \sin \alpha + \hat{k} \cos \alpha \quad (2)$$

where α is the angle between the +Z axis and a line to the observer.

The equation for the surface of the cone is given by:

$$x^2 + y^2 - \left(a - \frac{a}{h} z\right)^2 = 0 \quad (3)$$

A unit vector (\hat{n}) normal to S is given by:

$$\hat{n} = \nabla S / |\nabla S| \quad (4)$$

or, explicitly;

$$\hat{n} = \hat{i} x + \hat{j} y + \hat{k} m(a - mz) / \sqrt{x^2 + y^2 + m^2(a - mz)^2} \quad (5)$$

where $m = a/h$

The locus of points separating the illuminated and shadowed portions of the surface is given by setting:

$$\hat{n} \cdot \hat{l}_i = 0 \quad (6)$$

Using (1), (4), and (6), this locus is given by:

$$y \cos \beta - m(a - mz) \sin \beta = 0 \quad (7)$$

Similarly, the curve bounding the portion of the cone visible to the observer is given by setting:

$$\hat{n} \cdot \hat{u} = 0 \quad (8)$$

which from (2), (4), and (8) gives:

$$Y \sin \alpha + m (a - m z) \cos \alpha = 0 \quad (9)$$

At this point, it is convenient to go to cylindrical coordinates, recognizing that:

$$r^2 = x^2 + y^2$$

and the equation for the cone surface becomes:

$$r^2 - (a - m z)^2 = 0 \quad (10)$$

Then (7) can be rewritten as:

$$\sin \psi = m \tan \beta \quad (11)$$

or $\psi = \sin^{-1}(m \tan \beta)$, if $|m \tan \beta| \leq 1$.
If $|m \tan \beta| > 1$, the entire surface is illuminated.

Similarly, (9) can be rewritten as:

$$\sin \psi = -m \cot \alpha \quad (12)$$

or $\psi = \sin^{-1}(-m \cot \alpha)$ if $|m \cot \alpha| \leq 1$.
If $|m \cot \alpha| > 1$, the entire surface is visible to the observer.

Using the relationship given previously, we can compute the entire luminous flux to the observer by the integral:

$$F_o = 2 F_n \int_{z=0}^h \int_{\psi=\psi_1}^{\psi_2} \frac{(-\hat{l}_i \cdot \hat{n})(\hat{u} \cdot \hat{n})}{R^2} da$$

and $da = m(z - h) \sqrt{1 + m^2} d\psi dz$

The limits of ψ are:

$$\psi_1 = \left\{ \begin{array}{ll} \sin^{-1}(-m \cot \alpha) & \text{if } |m \cot \alpha| \leq 1 \\ -\pi/2 & \text{if } |m \cot \alpha| > 1 \end{array} \right\}$$

and

$$\psi_2 = \left\{ \begin{array}{ll} \sin^{-1}(m \tan \beta) & \text{if } |m \tan \beta| \leq 1 \\ \pi/2 & \text{if } |m \tan \beta| > 1 \end{array} \right\}$$

In this particular case using the dimensions of Figure A-1:

$$m \cot \alpha = 0.442$$

and

$$\psi_1 = \sin^{-1}(-0.442 \cot 57^\circ) = -25^\circ$$

The explicit form of the integral is rather complicated. Final integration was accomplished using a Gauss-Legendre double integration scheme as part of the computer program.

Analysis of the Cylinder

As before, the incident light comes from the direction defined by the unit vector ($\hat{\ell}_i$) which is given by (see Figure A-4):

$$\hat{\ell}_i = \hat{j} \cos \beta - \hat{k} \sin \beta$$

and the unit vector to the observer is given by:

$$\hat{u} = \hat{j} \sin \alpha + \hat{k} \cos \alpha$$

The unit vector normal to the surface is given by:

$$\hat{n} = \hat{i} \cos \psi + \hat{j} \sin \psi$$

In the case of the cylinder, the entire right half of the surface is illuminated and visible from $\beta = \pi/2$ to $\beta = 3\pi/2$. There is no contribution from the cylinder for other values of β .

Using the same premises as for the cone, the total luminous flux to the observer from the cylinder is:

$$F_o = 2 F_n \int_{z=0}^b \int_{\psi=0}^{\pi/2} \frac{(-\hat{l}_i \cdot \hat{n})(\hat{n} \cdot \hat{u}) da}{R^2}$$

where $da = a d\psi dz$

Explicitly:

$$F_o = \frac{2 a F_n}{R^2} \int_{z=0}^b \int_{\psi=0}^{\pi/2} (-\cos \beta \sin \psi)(\sin \alpha \sin \psi) d\psi dz$$

$$F_o = \frac{-a b F_n \cos \beta \sin \alpha}{R^2} \sqrt{\pi} \frac{\Gamma(3/2)}{\Gamma(2)}$$

$$F_o = - \frac{.886 \sqrt{\pi} a b F_n \cos \beta \sin \alpha}{R^2}$$

Projected Area of the Cone

As in the sphere case for the LEM, it was necessary to develop an expression for the projected areas of the cone and cylinder. The cone geometry may be found in Figure A-3. The observer is in a position defined by the unit vector:

$$\hat{u} = \hat{j} \sin \alpha + \hat{k} \cos \alpha$$

A unit vector (\hat{n}) normal to the surface of the cone is given by:

$$\hat{n} = \left(\hat{i} \cos \psi \cos \frac{a}{\sqrt{a^2 + h^2}} + \hat{j} \sin \psi \cos \frac{a}{\sqrt{a^2 + h^2}} + \hat{k} \sin \frac{a}{\sqrt{a^2 + h^2}} \right)$$

From the geometry:

$$\frac{a}{\sqrt{a^2 + h^2}} = \sin \left(\frac{\pi}{2} - \alpha \right)$$

Then:

$$\hat{n} = \hat{i} \cos \psi \sin \alpha + \hat{j} \sin \psi \sin \alpha + \hat{k} \cos \alpha$$

The projected area of the surface is given by:

$$\int \hat{u} \cdot \hat{n} \, da$$

where: $da = m(h-z)\sqrt{1+m^2} \, d\psi \, dz$

and: $m = a/h$

Performing the first integration:

$$A = 2 \int_{z=0}^h \int_{\psi=\psi_1}^{\psi_2} (\sin^2 \alpha \sin \psi + \cos^2 \alpha) m(h-z)\sqrt{1+m^2} \, d\psi \, dz$$

$$A = m h^2 \sqrt{1+m^2} \int_{l_1}^{l_2} (\sin^2 \alpha \sin \psi + \cos^2 \alpha) d\psi$$

45

$$A = m h^2 \sqrt{1+m^2} \left(\psi \cos^2 \alpha - \sin^2 \alpha \cos \psi \right) \Big|_{l_1}^{l_2}$$

Where the limits l_1 and l_2 are given by:

$$0 < \beta < \alpha \quad \begin{cases} l_2 = \sin^{-1}(m \tan \beta) \\ l_1 = -25^\circ \end{cases}$$

$$\alpha < \beta < \frac{\pi}{2} + \alpha \quad \begin{cases} l_2 = \pi/2 \\ l_1 = -25^\circ \end{cases}$$

$$\frac{\pi}{2} + \alpha < \beta < \pi + \alpha \quad \begin{cases} l_2 = \pi/2 \\ l_1 = \sin^{-1}(m \tan \beta) \end{cases}$$

$$\beta > \pi + \alpha \quad \begin{cases} l_1 = l_2 = A = 0 \end{cases}$$

The principles used to establish these limits are given in the section deriving the luminous flux from the cone.

Projected Area of the Cylinder

The geometry of the problem is shown in Figure A-4. As in the case of the cone, the projected area is given by:

$$A = \int_S \hat{u} \cdot \hat{n} da$$

Where as before:

$$\hat{u} = \hat{j} \sin \alpha + \hat{k} \cos \alpha$$

$$\hat{n} = \hat{i} \cos \psi + \hat{j} \sin \psi$$

$$da = a d\psi dz$$

Performing the integration:

$$A = 2 \int_{z=0}^b \int_{\psi=0}^{\pi/2} a \sin \alpha \sin \psi d\psi dz$$

$$A = 2 a b \sin \alpha$$

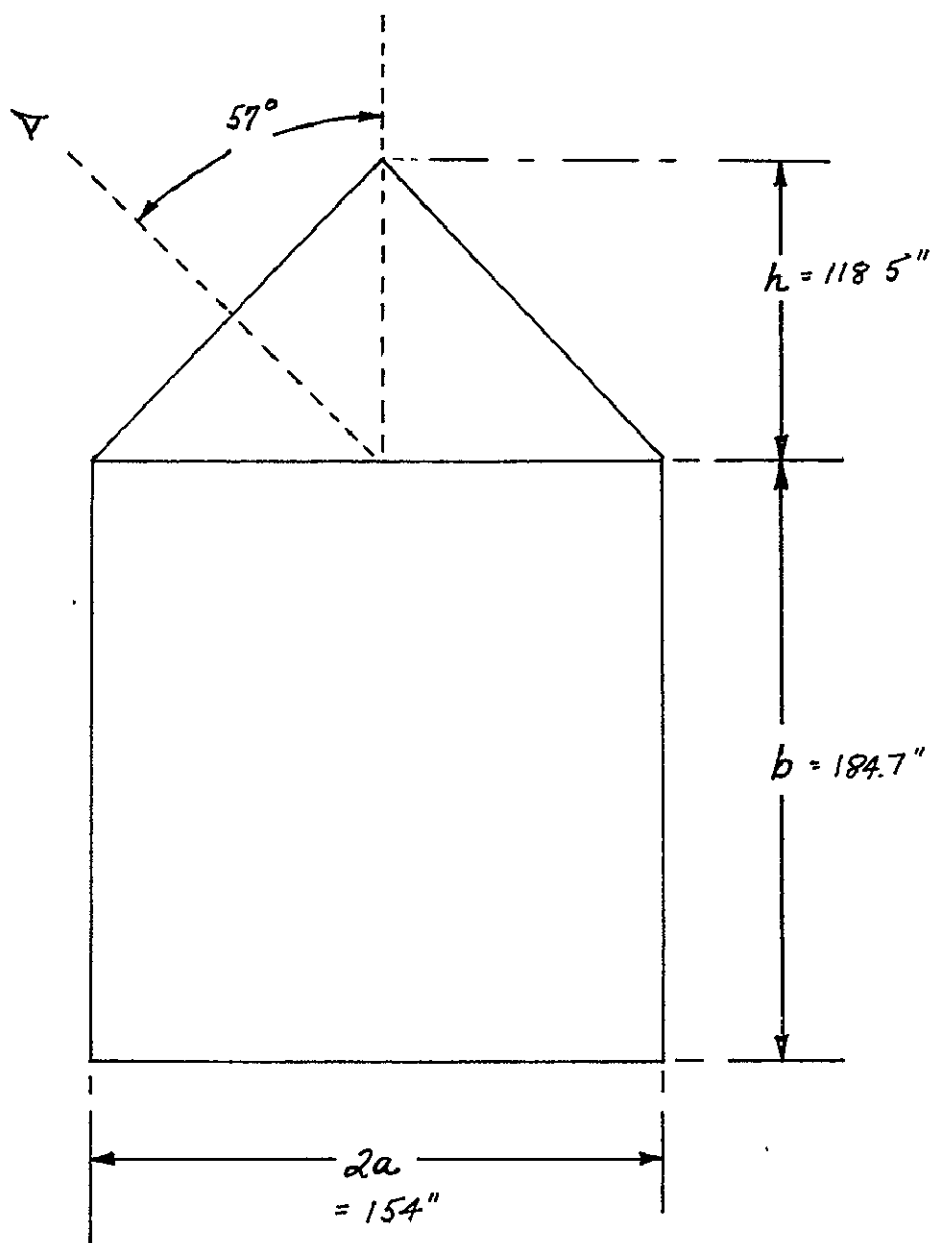


FIGURE A-1
CONE-CAPPED CYLINDER DIMENSIONS

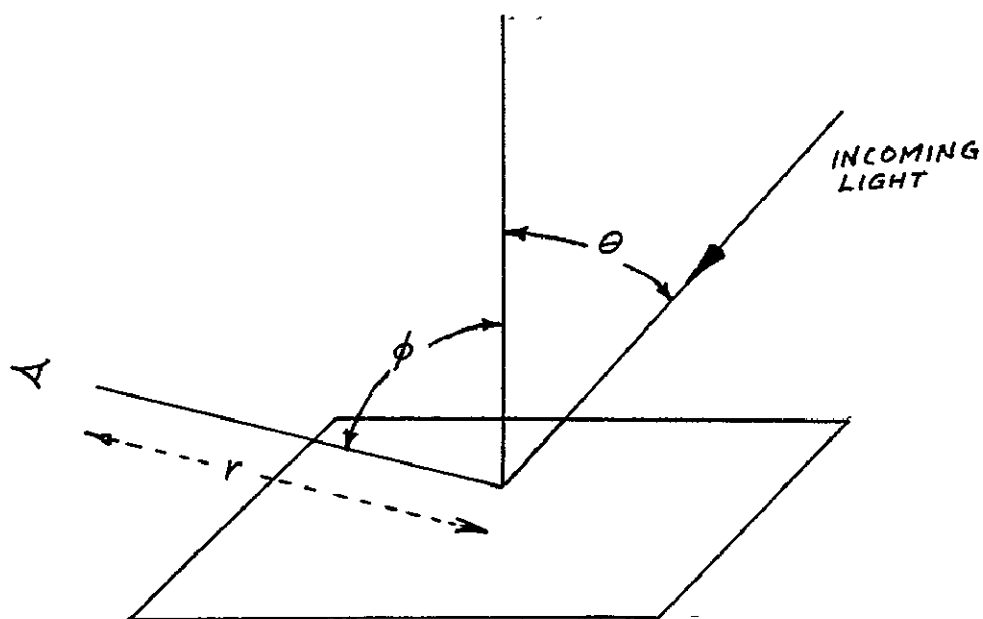


FIGURE A-2
DIFFUSE REFLECTION GEOMETRY

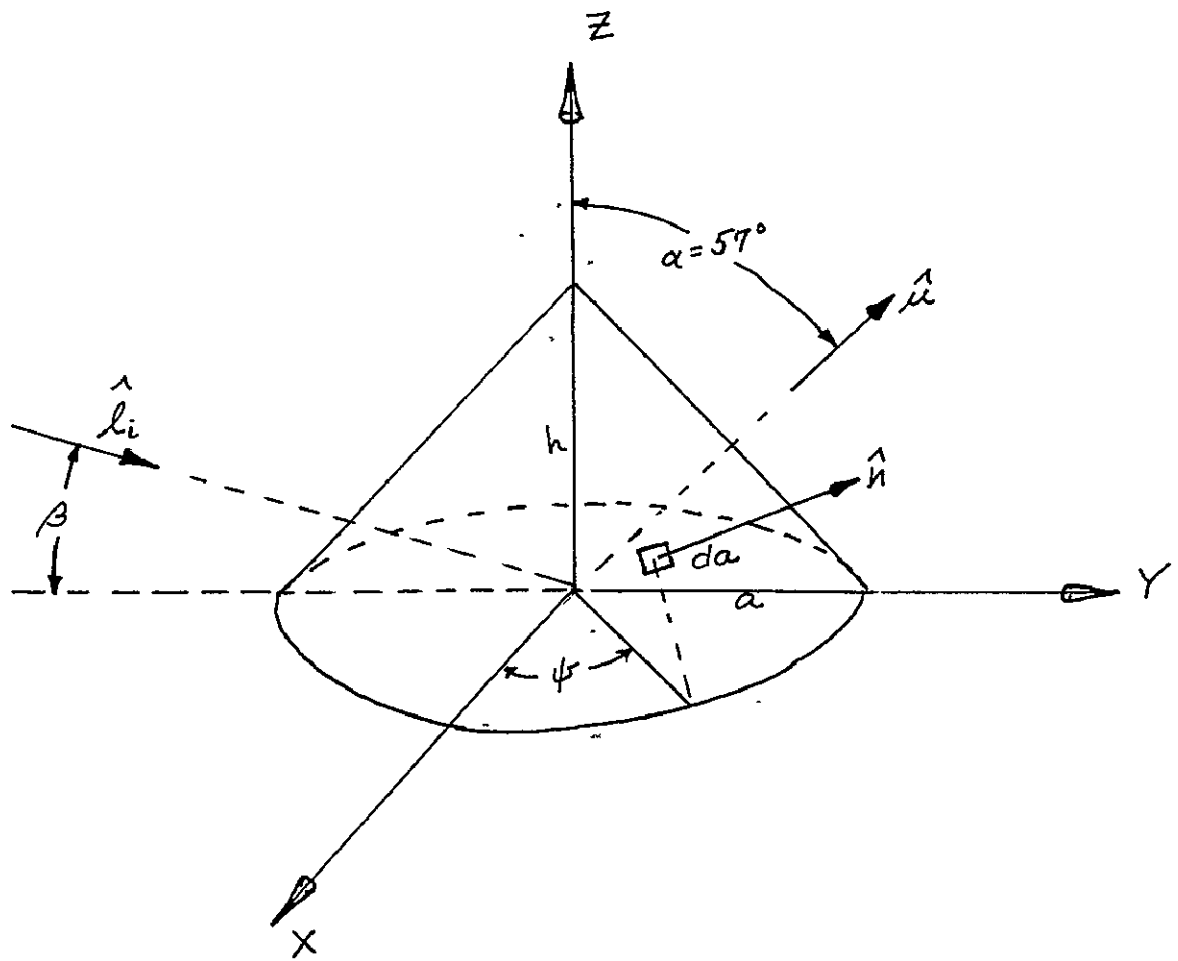


FIGURE A-3
CONE GEOMETRY

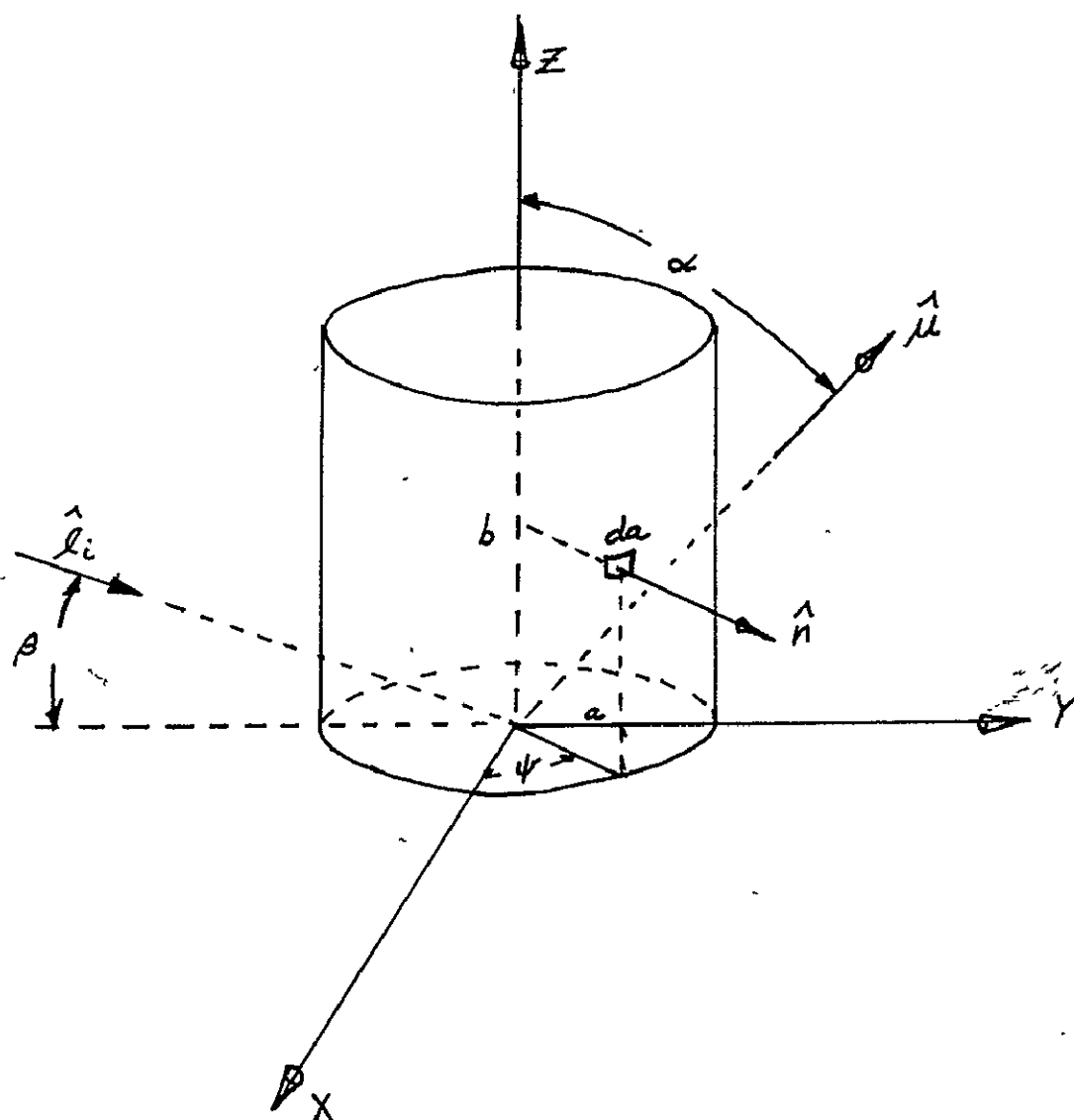


FIGURE A-4
CYLINDER GEOMETRY